Long Wavelength AC Bias Recording Theory

H. NEAL BERTRAM, MEMBER IEEE

Abstract—Long wavelength ac bias record sensitivity is computed utilizing a model in which both longitudinal and vertical record fields are considered. It is assumed that the recorded magnetization is related by an anhysteretic susceptibility tensor to the signal field. At each depth in the tape the signal field is evaluated where the bias field amplitude is equal to the tape coercivity. Neither the effects of demagnetizing fields nor spreads in particle switching fields are included. The calculation yields excellent quantitative agreement with experimental sensitivity and correlates well with the shape of measured sensitivity vs. bias curves. The predictions of this model are compared in detail with those calculated utilizing solely longitudinal fields.

INTRODUCTION

Audio tape recording is remarkable in that the desired system linearity is achieved by the superposition of a high frequency, large amplitude "ac bias" onto the record signal. The fundamental magnetic process is known as anhysteresis and may be measured on small samples of magnetic tape using ac and dc magnetizing fields. It is useful to relate basic magnetic tape properties, such as anhysteresis, to the ultimate recording performance. This not only helps to understand the process in detail, but allows one to distinguish between those effects which are inherent to the magnetic tape and those which are related to the recording field configuration. One method is to measure the anhysteretic magnetization and then, using the actual recording field geometry, calculate the tape flux which would result from the recording process. It is difficult to keep the calculation from becoming overly complicated since not only are the recording fields geometrically complex, but demagnetizing fields occur due to the spatially varying magnetization and concomitant imaging of such patterns in the record head. These modeling complexities are compounded when an attempt is made to calculate short wavelength performance. In fact, at short wavelength, detailed information about the anhysteretic process itself is required. Thus, most models have been restricted to utilization of only recording field components in the longitudinal direction parallel to the head-to-tape motion, and for the most part have neglected demagnetizing fields [1],[2]. To date, the various models have led only to good qualitative understanding of analog recording.

In this paper we would like to present a simple model which may be used to calculate the low-level long wavelength performance of ac bias recorders. It will be shown that excellent quantitative agreement may be achieved by neglecting demagnetizing fields but including both longitudinal and vertical recording fields. In the following sections, the basic anhysteretic process will be discussed followed by a description of the method of calculation using only longitudinal fields. The total field model will then be presented in two parts: first, assuming a negligibly small record gap length, an analytic formula will be derived which shows a clear improvement in correlation with experimental record sensitivity versus bias level; second, the more complex case of a finite gap will be presented in the form of numerically computed curves, since an analytic solution cannot be found.

Manuscript received July 1, 1974; revised August 13, 1974.
The author is with the Ampex Corporation, Redwood City, Cal. 94063.

THE ANHYSTERETIC PROCESS

An anhysteretic magnetization is developed in a material by the application of the time sequence of spatially uniform fields shown in Fig. 1. A large, high frequency bias field and low-level dc "signal" field are applied simultaneously; the ac field is reduced to zero while the dc signal field is held constant. The dc field is then removed and the remanent magnetization is measured. In Fig. 2a a typical anhysteretic magnetization curve is plotted against dc field. As is well known [3], it is necessary to have the initial ac amplitude at least as large as the coercivity to obtain appreciable magnetization. As the ac field is lowered and passes through the coercivity region, the magnetizing process occurs. The ac field provides only the switching energy for the particle magnetizations; given sufficient initial amplitude it does not affect the resultant magnetization. The anhysteretic magnetization is determined by a playoff of dc or signal field and interaction fields [4]. In fact, if there were no interactions, the process would yield only a saturated magnetization for any signal field value, rendering analog recording impossible.

It is interesting to compare the anhysteretic magnetization curve with the initial virgin remanence curve as shown in Fig. 2b. The benefits of including ac bias are obvious. The initial anhysteretic susceptibility, which is related to the recording sensitivity, is about a factor of twenty larger than the initial remanence susceptibility; the anhysteretic curve is single

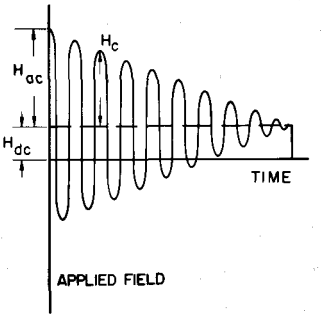

Fig. 1. Time sequence of total anhysterizing field: bias field (H_{ac}) and dc signal field (H_{dc}).

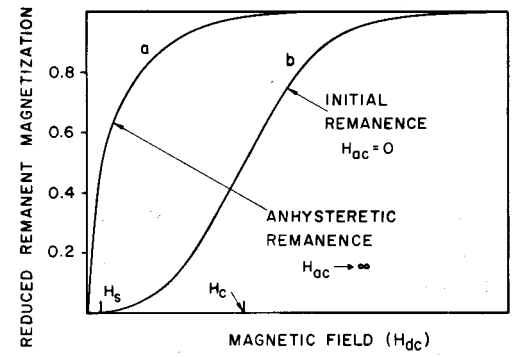

Fig. 2. Anhysteretic remanent magnetization (a) and initial remanent magnetization (b) vs. magnetizing field (H_{dc}). Magnetizations are normalized to saturation remanence. H_c denotes tape coercivity whereas H_s is a typical anhysterizing field.

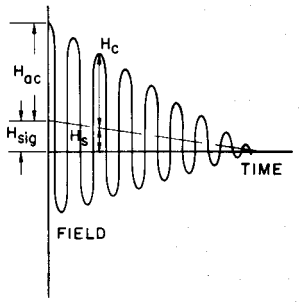

Fig. 3. Time sequence of total applied fields in modified anhysteretic process: bias field (H_{ac}) and peak signal field (H_{sig}). H_s is the effective signal field which induces the anhysteretic magnetization as given on Fig. 2a.

valued, whereas the remanence curve exhibits hysteresis depending strongly on the field history. Nonlinearity (related to third harmonic distortion) becomes appreciable at about the 40% magnetization level in anhysteresis, whereas significant nonlinearities set in immediately in the initial remanence curve.

Initial anhysteretic susceptibilities $\chi \equiv dM/dH$ measured in the oriented direction typically fall in the range from 10 to 40.[1] The susceptibilities are a strong function of orientation so that unoriented samples exhibit susceptibilities near 10, whereas oriented samples show susceptibilities of 30-40. Co-doped γFe_2O_3 behaves like unoriented γFe_2O_3 so that its susceptibility is always about 10-20. Measured susceptibilities seem to be independent of coercivity, but not necessarily of the tape remanent magnetization M_r: if M_r is varied by tape loading then the susceptibility varies with M_r; whereas if M_r is varied by changing the intrinsic particle moment, then only slight variations are expected [4].

MODIFIED ANHYSTERETIC PROCESS

The time sequence of fields which define the modified anhysteretic process is shown in Fig. 3. It is more directly related to recording since both the dc and ac fields are decreased together. This process resembles the field sequence which a tape element sees as it passes the gap of a record head.

[1] MKS rationalized system of units is employed throughout in which $B=\mu_0(H+M)$.

Modified anhysteresis is virtually identical to the basic anhysteretic process except that the effective signal field which determines the final magnetization is the value of the decaying dc field when the ac field has been reduced to approximately the coercivity of the material. Thus, the modified anhysteretic magnetization curve is about the same as the ideal curve exhibited in Fig. 2a where the effective magnetizing field is the field H_s (Fig. 3). Since bulk material major loops are not square and possess moderately wide spreads in switching fields (Fig. 4) the anhysteretic process is a little more complex than the explanation given here. For long wavelength signals (or dc fields) the difference is small since the effective signal field does not vary appreciably over the coercivity range. However, for short wavelength signals it is possible for the signal field to change sign while the bias field amplitude is passing through the material coercivity range ($H_2 \rightarrow H_1$) resulting in a greatly reduced average signal field and thus yielding much smaller magnetizations. This is illustrated in Fig. 5.

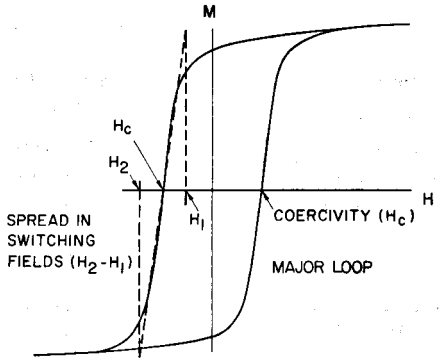

Fig. 4. Major loop of typical tape material.

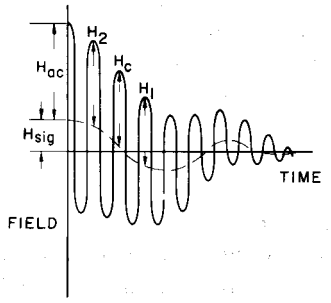

Fig. 5. Time sequence of total applied field in modified anhysteretic process for a short wavelength signal: bias field (H_{ac}) and signal field (H_{sig}).

In the modified process in uniform fields, the phenomenon of overbiasing is evident. For a fixed initial signal field amplitude, an increase in initial ac field amplitude results in lower effective signal fields and hence reduced magnetizations. One could follow this argument through for the whole bias field range and see a bias optimization for peak output. This is not to be confused with the bias optimization as measured on a recorder since, as will be discussed, a different effect, due to field nonuniformities, is occurring.

LONGITUDINAL LONG WAVELENGTH RECORDING MODEL

In the subsequent discussions, the usual two-dimensional approximation will be made: recording track edge effects will be neglected so that fluxes generated in the tape will be identical in every plane which includes the head-to-tape motion direction and the vertical to the tape surface. Thus, all fluxes computed will be flux per unit width of track. Since only long wavelength, linear recording is being discussed, it is sufficient to consider only peak signal fields: the time variation of the resultant recorded magnetization will be taken to be the same as that of the recording signal. The magnetic fields generated by the head will be assumed to be of the Karlqvist form [5]:

$$H_x = \frac{H_0}{\pi}\left(\tan^{-1}\left(\frac{x+g/2}{y}\right) - \tan^{-1}\left(\frac{x-g/2}{y}\right)\right) \tag{1}$$

$$H_y = \frac{H_0}{2\pi} \ln\left(\frac{(x-g/2)^2+y^2}{(x+g/2)^2+y^2}\right) \tag{2}$$

$$H_0 = \frac{NI}{g} \tag{3}$$

where g is the gap length and H_x, H_y are, respectively, the longitudinal and vertical field components. H_0 is the deep gap magnetic field which is a function of the head current, I, the number of turns, N (either signal or bias), and the gap length g (assuming a 100% efficient head). The Karlqvist approximation is reasonable at distances of $g/10$ or more from the head surface.

For computational ease the tape coercivity is taken to be isotropic. As mentioned, the effects of a range in switching fields will not be considered. It is assumed that the bias is of infinite frequency so that the magnetizing occurs precisely when any given tape element sees a decreasing bias field amplitude equal to its coercivity. The resultant magnetization will be taken to be the anhysteretic magnetization of the specimen as shown in Fig. 2a which might be determined, for example, with a vibrating sample magnetometer.

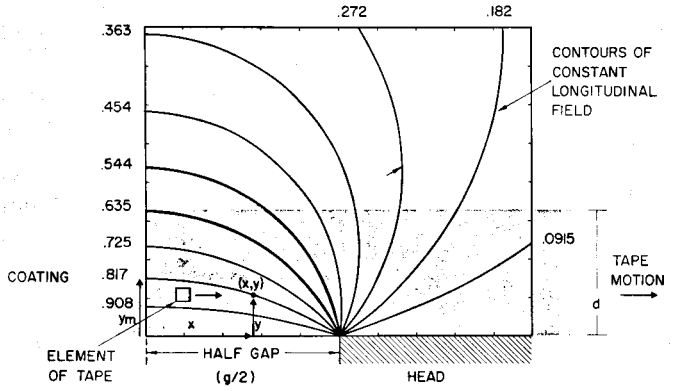

Fig. 6. Contours of constant longitudinal field in region above recording head surface. Left-hand edge is gap centerline. Contour magnitudes are in fraction of deep gap field. Tape magnetic coating is shaded with a typical element of tape demarked for text discussion of magnetizing process.

In this section, recording with only the longitudinal fields (H_x) will be considered. Figure 6 illustrates contour plots of constant longitudinal head field. The left-hand edge is the gap center line whereas the hatched region is the downstream core material. Since recording occurs while the bias field is decreasing, it is sufficient to consider only this field region. A contour labeled (for example) 0.817 means that the field everywhere along that line in the space above the head is equal to 0.817 H_0 whether H_0 is due to bias or signal current. The shaded region denotes the tape coating. The effect of head-to-tape spacing in the recording process will not be considered. Its inclusion is a trivial addition in any of the models presented and since spacings are usually only about 0.2 μm a negligible contribution is expected to the fluxes calculated herein.

Let a bias current of essentially infinite frequency and a very long wavelength signal current be applied. Further, let the bias current be initially such that the 0.817 contour field magnitude is equal to the tape coercivity. As the tape element shown in the figure crosses the 0.817 contour, at point (x,y), it is anhysterized by the modified process so that it leaves the contour with a magnetization

$$M = M_{ar}(H_s) \tag{4}$$

where $M_{ar}(H_s)$ is the anhysteretic magnetization due to an effective dc signal field H_s (Fig. 2a). Since only low level recording is being considered

$$M = \chi H_s \tag{5}$$

where χ is the longitudinal anhysteretic susceptibility and the effective signal H_s is the field corresponding to the 0.817 contour. It is important to emphasize that the same contours apply for both signal and bias. Thus, the simple relation

$$H_s = H_c \cdot H_0^s / H_0^b \tag{6}$$

holds where H_0^s, H_0^b, H_c are, respectively, the deep gap signal field, deep gap bias field, and tape coercivity. Further, any element of tape at any distance from the head less than the furthest extent of the 0.817 contour develops the same magnetization. In this model H_s is constant along any bias contour. For elements beyond the penetration depth of the 0.817 contour there is no magnetization recorded since with no switching field spread, as assumed in this model, there is insufficient bias field. The net flux amplitude in the tape is (per unit width), therefore

$$\phi = \mu_0 \chi H_s y_m \tag{7}$$

where y_m is the depth of the contour. This simple form for the flux is sufficient at long wavelengths since phase displacement through the depth of the recorded layer is unimportant. From Eq. 1, it can be shown easily that

$$y_m = \frac{g \cot\left(\frac{\pi H_c}{2H_0^b}\right)}{2} \tag{8}$$

Consider now the effect of increasing the bias current. Suppose that the 0.725 contour now corresponds to a bias

field magnitude equal to the tape coercivity. The previous argument holds except the recording contour is different. The net magnetization recorded for any tape element intercepting this contour is again equal to the anhysteretic susceptibility times the signal field along that contour. Since the signal current is assumed constant it is obvious that the effective recording field in this modified process is less than that in the previous case (Eq. 6 shows this directly). Thus the recorded magnetization is less, although the 0.725 contour extends further into the tape than the previous contour. However, the total flux (and hence replay voltage) increases since the increase due to the extended recorded flux penetration (y_m) outweighs the decreased recorded magnetization (M).

Further increases in bias current cause the flux to increase until the 0.635 contour, in this example, becomes the one with bias field equal to the coercivity. At this point, the flux no longer increases with increasing bias current since the entire depth of the coating is fully recorded. For additional bias increases the depth of recording y_m remains equal to the coating thickness d. Thus, the flux now decreases with increasing bias current since the effective signal is changing, and, as Eq. 6 shows, the recording signal decreases with increasing bias. It should be emphasized that the contours and tape coating in Fig. 6 are entirely arbitrary and are for discussion purposes only; it is entirely coincidental that the 0.635 contour penetrates first to the back of the coating.

The bias to achieve maximum output or record sensitivity is seen clearly to occur when the recording has just penetrated to the back of the tape coating. Bias optimization of recorded flux is due to a play-off of effective signal field and depth of recording. It is not directly caused, as indicated by discussion of the modified anhysteretic process, by a play-off of decreasing effective signal field and increasing bias amplitude. At each depth in the tape where recording occurs there is always sufficient bias amplitude. The only connection is that an increasing bias provides for a deeper recording penetration since the fields decay spatially away from the head surface.

Using the previous equations, expressions for the tape flux at all bias levels may be listed:

Under bias:

$$\phi = \frac{\mu_0 \chi N I_s}{\pi} \cdot \frac{\pi H_c \operatorname{cotan}\left(\frac{\pi H_c}{2H_0^b}\right)}{2H_0^b}. \tag{9}$$

Over bias:

$$\phi = \frac{\mu_0 \chi N I_s}{\pi} \cdot \frac{\pi d H_c}{g H_0^b}. \tag{10}$$

Optimum bias (maximum record sensitivity):

$$\phi = \frac{\mu_0 \chi N I_s}{\pi} \cdot \frac{2d \tan^{-1}\left(\frac{g}{2d}\right)}{g}. \tag{11}$$

The current at optimum bias is,

$$I_b = \frac{\pi H_c g}{2N \tan^{-1}\left(\frac{g}{2d}\right)}. \tag{12}$$

These expressions may be expressed in different forms by utilization of Eq. 3, which relates the deep gap signal or bias field to the respective driving current. In Fig. 7, plots of reduced output flux for fixed signal current I_s (record sensitivity) versus bias level for various coating thickness to gap length ratio (d/g) are shown. The curves replicate essentially Fig. 3 of Ref. [2] and explain the basic features of long wavelength recording. The locus of maxima is just Eq. 9 which is independent of both the gap length and coating thickness. In this model, the bias for maximum sensitivity is reached abruptly for each coating thickness to gap ratio (d/g) when Eq. 11 holds. Thereafter, the level decreases with bias current according to Eq. 10. If the effect of nonsquare loops (distribution in switching fields) is included, then the peaks are flattened somewhat and the decrease in flux upon lowering the bias below optimum is not so precipitous. The curves of Daniel and Levine [2] are smooth near bias optimization since in their work the effect of a spread in switching fields on the anhysteretic process has been included empirically. It should be emphasized that the longitudinal model predicts correctly that the bias curves scale with tape coercivity and that the maximum sensitivity occurs for a bias that just records through to the back of the tape. This behavior is experimentally verifiable and will not be altered theoretically by a total field model, certainly as long as demagnetizing fields are neglected.

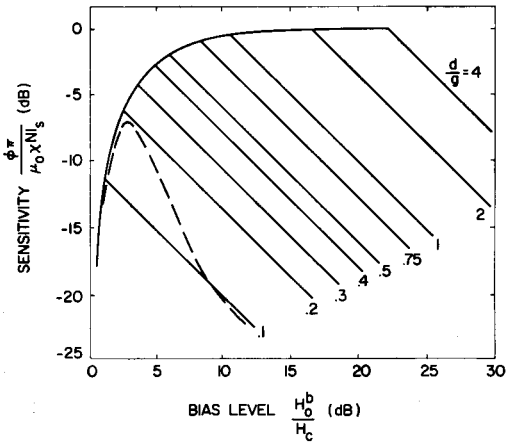

Fig. 7. Output vs. bias for various coating thickness to gap ratios (d/g) using longitudinal model. Dashed line is data for a γFe_2O_3 tape placed to match peak output point.

There are two difficulties with the predictions of this model. In Fig. 7, we show a measured output versus bias curve, measured on a γFe_2O_3 tape with d/g = 0.2, which has been shifted vertically and horizontally to match the simple theory as well as possible. Whereas the curves match reasonably well below optimum bias conditions, the over bias behavior differs significantly. Further, as noted by Daniel and Levine [2], and observed by us, the calculated maximum flux using measured anhysteretic susceptibilities is typically about a factor of two higher than that measured

with calibrated record and reproduce heads. Both these difficulties may be easily remedied by using a slightly more complex model which considers both longitudinal and vertical recording fields.

TOTAL FIELD MODEL

Utilization of both vertical and longitudinal recording fields renders the flux expression quite complex. However, in the limit of short recording gaps it is possible to give the flux in analytic form. We consider first this limit and then show computer generated curves for several finite gap-to-coating thickness ratios.

Zero Gap Length Limit

Equations 1, 2, and 3 simplify in the limit of negligible gap to the expressions

$$H_x = \frac{NIy}{\pi r^2} \tag{13}$$

$$H_y = \frac{NIx}{\pi r^2} \tag{14}$$

and

$$H \equiv \sqrt{H_x^2 + H_y^2} = \frac{NI}{\pi r} \tag{15}$$

where the coordinates x, y and $r = \sqrt{x^2 + y^2}$ are illustrated in Fig. 8. The contours of constant total field are circles centered at the top of the gap. Recording occurs, as in the previous discussion, just as elements of tape pass the "downstream" edge of the bias contour corresponding to the tape coercivity for any given bias current. It is assumed that the bias field direction is irrelevant. The magnetization which results is now slightly more complex. We assume that the low level anhysteretic process may be described by a diagonal tensor susceptibility

$$\overleftrightarrow{\chi} = \begin{pmatrix} \chi_x & 0 \\ 0 & \chi_y \end{pmatrix} \tag{16}$$

so that

$$M_x = \chi_x H_x^s \tag{17}$$

$$M_y = \chi_y H_y^s \,. \tag{18}$$

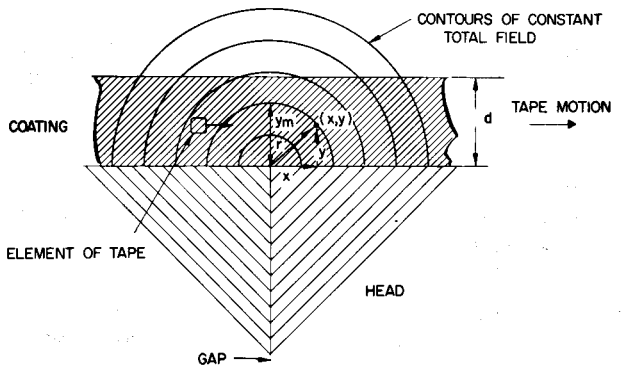

Fig. 8. Contours of constant total field for "zero gap" head.

In this approximation χ_x can be taken to be the anhysteretic susceptibility measured in the longitudinal or orientation direction whereas χ_y is that measured vertically. Thus χ_x is identical to the χ utilized in the longitudinal model.

In the previous discussion the fields were solely longitudinal so that $H_x^s = H_s$ was constant along the bias contour equal to the coercivity. This is no longer true in a total vector field model. Since recording always occurs along the contour of total bias field equal to the coercivity, the longitudinal (H_x^s) and vertical (H_y^s) field components vary along the recording contour. If the bias is set at a value I_b, then from Eq. 15 the furthest penetration of the coercivity contour is

$$y_m = \min\left(d, \frac{NI_b}{\pi H_c}\right) \tag{19}$$

The magnitude of the flux is given by

$$\phi = \sqrt{\phi_x^2 + \phi_y^2} \tag{20}$$

where

$$\phi_x = \mu_0 \int_0^{y_m} \chi_x H_x^s(y)\,dy \tag{21}$$

$$\phi_y = \mu_0 \int_0^{y_m} \chi_y H_y^s(y)\,dy \,. \tag{22}$$

The integrals are taken along that section of the coercivity contour where anhysteresis occurs. The appropriate path is from the downstream end of the contour (where it meets the tape surface) back into the tape to the point of furthest penetration. ϕ_x, ϕ_y are not vector components but the flux due, respectively, to longitudinally and vertically recorded magnetizations. Equation 20 is the proper form for the total flux since at any wavelength, the two components of recorded flux are reproduced in phase quadrature. Along the contour Eqs. 13-15 hold so that integration readily yields:

$$\phi_x = \frac{\mu_0 \chi_x NI_s}{2\pi}\left(\frac{y_m H_c \pi}{NI_b}\right)^2 \tag{23}$$

$$\phi_y = \frac{\mu_0 \chi_y NI_s}{2\pi}\left\{\sin^{-1}\left(\frac{y_m H_c \pi}{NI_b}\right) + \frac{1}{2}\sin\left[2\sin^{-1}\left(\frac{y_m H_c \pi}{NI_b}\right)\right]\right\} \tag{24}$$

Case 1

Under Bias: $y_m = \dfrac{NI_b}{\pi H_c} \leqslant d \,.$

Evaluation of Eq. 20 with Eqs. 23 and 24 yields

$$\phi = \frac{\mu_0 \chi_x NI_s}{2\pi}\sqrt{1 + \left(\frac{\pi \chi_y}{2\chi_x}\right)^2} \tag{25}$$

Since the limit of infinitesimal gap has been considered, the output is constant up to the "peak bias" condition

($y_m = NI_b/\pi H_c = d$). This occurs since the deep gap field is arbitrarily large for any bias current. For well oriented tape, the longitudinal susceptibility (χ_x) is much larger than the vertical component. Thus,

$$\phi \cong \frac{\mu_0 \chi_x NI_s}{2\pi}. \tag{26}$$

This is to be compared to that previously derived utilizing the longitudinal model (Eq. 11) which becomes in the zero gap limit:

$$\phi = \frac{\mu_0 \chi NI_s}{\pi}. \tag{27}$$

The only difference is the factor of one-half entering the flux expression calculated using the total field model. The flux is reduced since the longitudinal recording field averaged over the total field bias contour is less (it vanishes near the tape surface) than along a bias contour of longitudinal field. The experimental corroboration of this prediction is seen clearly upon examination of Table I. This table is a compilation of results from Ref. [2]. It is striking that the experimental sensitivities are all about a factor of two below the theoretical predictions of a longitudinal model. In fact, the ratios are, for the most, slightly larger than a factor of two. In the next section, it will be shown how a consideration of a finite gap length ($g > 0$) improves the experimental corroboration.

It is illustrative to compare the distribution of recorded magnetization in the tape for the two models in the limit of zero gap at optimum bias. In the longitudinal model, the magnetization is uniform throughout the coating and is given (e.g., by inference from Eq. 27) by

$$M_x = \frac{\chi_x NI_s}{\pi d}. \tag{28}$$

In the total field model, the longitudinal and vertical components of magnetization are given (e.g., utilizing Eqs. 13, 14, 17, 18 with $y_m = r = d$) by

$$M_x = \frac{\chi_x NI_s y}{\pi d^2} \tag{29}$$

$$M_y = \frac{\chi_y NI_s}{\pi d}\sqrt{1 - \left(\frac{y}{d}\right)^2}. \tag{30}$$

These magnetizations are plotted in Fig. 9 in which, for illustration, it is assumed that $\chi_y/\chi_x = 0.20$. In the total field model, the longitudinal component vanishes at the surface and increases linearly until it is equal at the back of the tape to the magnitude predicted by the longitudinal model. This coincidence occurs since at the depth of furthest recording penetration, the bias and signal fields are both longitudinal. The vertical component is largest at the tape surface and gradually decreases and vanishes at the back of the coating. This behavior has been seen and qualitatively explained by Tjaden and Leyten [6]. The measured magnetization patterns presented in their Fig. 14 are very similar to those plotted here in Fig. 9.

Case 2

$$\text{Over Bias:} \quad y_m = d \leqslant \frac{NI_b}{\pi H_c}.$$

The purely longitudinal theory predicts that the flux decreases inversely with increasing bias in the over biased region. Equation 10 exhibits this relation explicitly. In the total field model, the variation is different and is given by Eqs. 23 and 24. In Fig. 10 the normalized variation of ϕ_x in Eq. 23 and ϕ_y in Eq. 24 are plotted vs. reduced bias current.

TABLE I
COMPILATION OF RECORDING DATA FROM REFERENCE [2]

TAPE	d/g*	H_c (Oe)**	B_r(G) ***	Relative Sensitivity		
				Longitudinal Theory	Experiment	Ratio Th/Exp.
A	.128	245	745	4.41	2.18	2.02
B	.264	254	1050	10.16	4.43	2.29
C	.273	251	1190	14.5	5.02	2.89
D	.290	260	732	6.65	3.36	1.98
E	.290	250	1110	12.7	5.08	2.50
F	.341	275	797	7.09	3.74	1.89
G	.400	270	865	9.88	4.35	2.27
H	.400	250	823	11.6	4.67	2.48
I	.443	253	734	8.73	3.97	2.20
J	.443	247	783	12.3	4.71	2.61
K	.469	263	860	9.11	4.46	2.04
L	.477	263	850	8.24	3.98	2.07
M	.656	245	1100	23.9	6.99	3.42

* Coating thickness to gap ratio.
** 1 Oe is equivalent approximately to 80 A/M.
*** 1 G is equivalent to 10^{-4} Tesla.

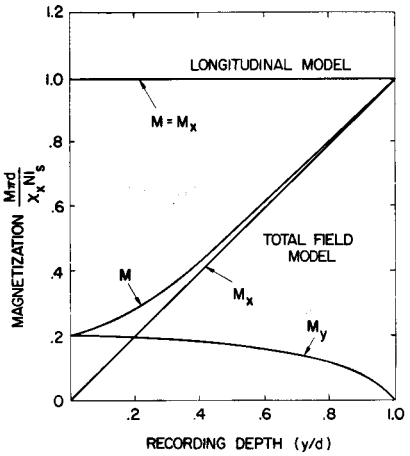

Fig. 9. Recorded magnetization vs. depth into tape for longitudinal and total field models. The bias has been set to record through to the back of the coating. The zero gap length limit is considered for both models.

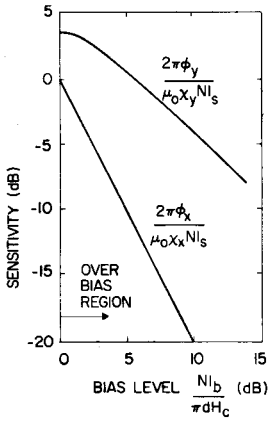

Fig. 10. Tape flux vs. bias due to longitudinally (x) and vertically (y) recorded magnetization components by a zero gap length record head. 0 dB bias denotes maximum sensitivity from recording through to the back of the tape coating.

In contrast to a purely longitudinal model the flux from longitudinally recorded magnetization ϕ_x decreases quadratically with bias. The vertical flux contribution ϕ_y varies slowly with bias at first and inversely for large bias current ($NI_b/\pi H_c \gg d$). Since, in general, tape is well oriented so that $\chi_y \ll \chi_x$, the flux from the longitudinal magnetization dominates the total flux when the bias current is not too much greater than optimum. Thus, this model predicts that the flux will vary beyond optimum, initially, as the square inverse of the bias current (I_b). As the bias is increased substantially past optimum, the dominant longitudinal flux contribution begins to diminish rapidly according to its inverse quadratic bias dependence. Even though the vertical flux contribution is small, it decreases inversely so that at some bias value the longitudinal contribution becomes smaller than the vertical flux contribution yielding a flux which varies inversely with bias. This behavior is seen in Fig. 7 in which an experimental output versus bias curve is shown superimposed on the results for the purely longitudinal field model.

It is interesting to note that the inverse bias dependence at high bias for the total field model is the same variation as predicted by the longitudinal model for any bias past optimum. In this limit, Eq. 24 becomes

$$\phi_y = \mu_0 \chi_y H_c d\,(I_s/I_b)\,. \tag{31}$$

This is identical in form to Eq. 10 which yields utilizing Eq. 3:

$$\phi = \mu_0 \chi H_c d\,(I_s/I_b)\,. \tag{32}$$

The reason is that at large bias fields the total field is essentially vertical with negligible longitudinal contribution. Thus, in this limit, as in the longitudinal model, contours of constant bias field are also contours of constant signal field.

It might be expected for isotropic systems ($\chi_x = \chi_y$) that Eqs. 23 and 24 should simplify to yield a flux which would vary inversely with bias for all bias values beyond optimum. Even though bias contours would coincide with signal contours, the 90° phase shift between the reproduced flux of the longitudinally recorded magnetization ϕ_x and its vertical counterpart ϕ_y prohibits such a simplification. However, as will be shown in the next section, the inverse bias dependence is exhibited theoretically to good approximation.

Finite Gap Lengths

To determine the recorded flux for a finite gap, it is necessary to evaluate Eqs. 21 and 22 utilizing the general form of the fields H_x^s, H_y^s from Eqs. 1 and 2. The integration is again along the "downstream" side of a contour of total field equal to the coercivity. In Fig. 11, the contours of constant total field near the gap are displayed. Equations 1 and 2 were used to determine the field. The contours tend to become circular at distances far from the gap since this figure is just a magnification of Fig. 8 in the region near the gap. Very close to the gap the contours tend to cluster around the gap edge with maximum field penetration for any given contour being near the gap edge rather than along the gap centerline.

In Fig. 12, computed low level sensitivity vs. bias curves are displayed for $d/g = 0.2$, $\chi_x = 31.4$, $\chi_y = 6.28$, 2.0 and 0.0. The anhysteretic values are typical for oriented γFe_2O_3 tape measured in the orientation direction ($\chi_x = 31.4$) and planar transverse ($\chi_y = 6.28$). The curves for $\chi_y = 2.0$, 0.0 are shown

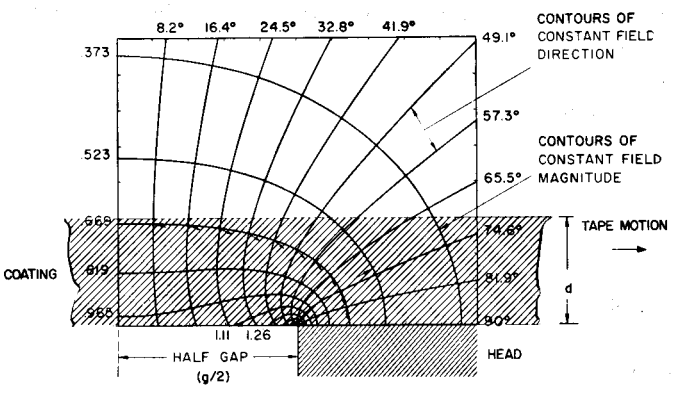

Fig. 11. Contours of constant total field and field direction. Head is same as in Fig. 6 except here field direction contours are shown where angle is deviation down from horizontal (explicitly shown on contour 0.669).

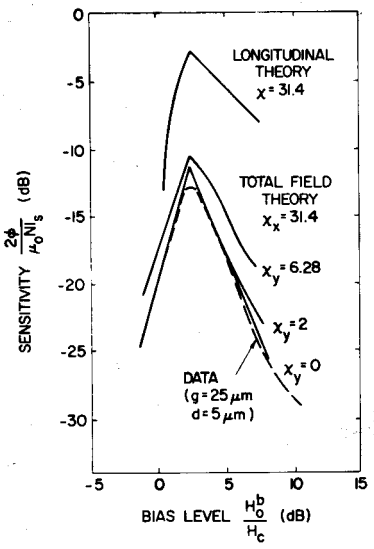

Fig. 12. Sensitivity vs. bias field from total field model for $d/g = 0.2$ for longitudinal anhysteretic susceptibility $\chi_x = 31.4$ and various vertical components χ_y. Longitudinal theory result from Fig. 6 is shown for comparison.

to simulate one effect of demagnetizing fields since the important transverse direction is perpendicular to the tape plane. The result for the longitudinal theory (Fig. 7 $d/g = 0.2$) is shown also (where $\chi = \chi_x = 31.4$). Since all the curves scale with tape coercivity the bias level is just the deep gas bias field relative to a particular tape coercivity. Equation 3 can be used to relate the peak bias current to the deep gap bias field.

All curves show maximum sensitivity at about the same bias. This is true for all values of $d/g > 0.1$ where the deepest tape penetration is along the gap centerline. The field is purely longitudinal along this head symmetry plane so that the optimum bias argument holds for both models. Optimum sensitivity in the total model has been reduced about 8.5 dB (a ratio of about 2.5) from that predicted by a purely longitudinal model; this is in better agreement, on the average, with the results of Ref. [2], presented in Table I, than the zero gap result. Further, it is seen, as predicted by Eq. 25, that since $\chi_x \gg \chi_y$, the influence of χ_y on peak sensitivity is small. χ_y does influence the over bias sensitivity in agreement with Eq. 24. Larger χ_y tend to dominate the output sooner as the bias is increased so that the inverse output versus bias region is reached sooner. In the longitudinal model (with no spread in switching fields) there is no flux for a bias level less than 0 dB since that is the level where field penetration into the tape just begins. However, for the total field model there is always some field penetration (Fig. 10), however small, so that no minimum bias cutoff exists.

The same experimental curve for $d/g = 0.2$ which was shown in Fig. 7 is plotted here in Fig. 12. Since the record head was not calibrated the curve is again shifted for a best fit. The corroboration of the output versus bias curve with that predicted by a total field theory is striking. Both the measured curve and theoretical curves exhibit the same quadratic decrease of flux with bias just past optimum. For extreme over bias the measured flux curve changes shape to vary approximately inversely with bias as predicted. However, none of the calculated curves, or possible variations with different vertical anhysteretic susceptibility (χ_y), can fit the precise shape of the measured curve over the total bias range.

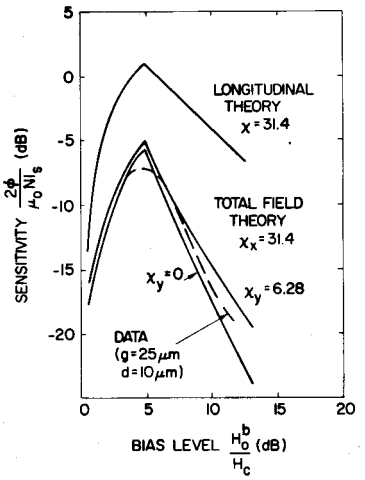

Fig. 13. Sensitivity vs. bias field from total field model for $d/g = 0.4$ for longitudinal anhysteretic susceptibility $\chi_x = 31.4$ and various vertical components χ_y. Longitudinal theory result from Fig. 6 is shown for comparison.

In Fig. 13, calculated results are shown for a coating thickness to gap length ratio of $d/g = 0.4$. The curves are basically the same but a bit broader since more bias is required to record to the far side of the tape coating. The flux difference at peak bias between the two models (for $\chi_y = 0.0$) is now only 7.5 dB. This difference approaches the analytic result of 6 dB for zero gap. The data shown are again a "best positioning" of output versus bias for a γFe_2O_3 tape of 10 μm coating recorded by a head of 25 μm gap length. The curve shape matches theory quite well using the total field model whereas again it is obvious the fit is poor using the purely longitudinal model.

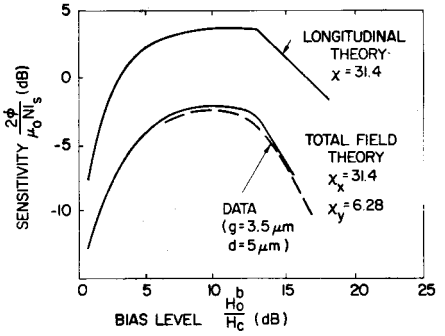

Fig. 14. Sensitivity vs. bias from total field model for $d/g = 1.43$ for longitudinal anhysteretic susceptibility $\chi_x = 31.4$ and vertical component $\chi_y = 6.28$. Longitudinal theory result from Fig. 6 is shown for comparison.

In Fig. 14, computed output versus bias curves for a record gap smaller than the coating thickness ($g = 3.5$ μm, $d = 5$ μm) are shown. As expected the high d/g ratio yields very broad curves. The experimental data again support the total field model. In Fig. 15, the results of both models are plotted for an isotropic tape. It is interesting that the calculated peak fluxes coincide for optimum and overbias. This

can be seen by comparing Eqs. 25 and 27 even though they were calculated in the zero gap limit.

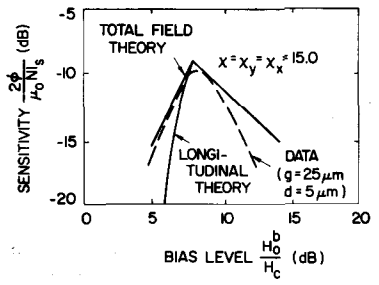

Fig. 15. Sensitivity vs. bias from total field model for $d/g = 0.2$ for equal anhysteretic susceptibilities $\chi_x = \chi_y = 15.0$. Longitudinal theory result from Fig. 6 is shown for comparison.

Under bias the total field model yields more output since, as discussed previously, the total field penetrates further into the coating for low bias values. At high bias, the curves coalesce with the total field model exhibiting an inverse bias dependence. Anhysteretic isotropy in the total field model renders bias and signal contours coincident. Even though the recorded magnetization is thereby uniform along the recording contour, the relative flux contribution to vertical and longitudinal components is changing. In spite of this complication, the computed output gives very closely the simple inverse dependence. A measured curve using nominally isotropic Co–γFe_2O_3 is shown for comparison in Fig. 15. Even though the low bias shape follows the total field model, the over bias shape is more like that expected from an oriented tape. This results most likely from demagnetization of the vertical anhysteretic component so that χ_y is always near zero.

It should be emphasized that all the data shown are for comparison with predicted curve shape. The absolute comparison of peak sensitivity is only via the data of Ref. [2] where calibrated recorded and replay systems were utilized.

DISCUSSION

Utilization of the total vector field in the recording model entails the existence of vertically recorded magnetization. As mentioned, such components have been seen [6]; however, it may be inferred from this study that, for well oriented tapes at least, their magnitude is quite small. In long wavelength bias recording they affect the output flux appreciably only in the region of extreme overbias. Thus, to good approximation, over most bias values a reasonable model could include the total vector field for the bias but only the longitudinal component of the signal field. Neglecting the vertical component of the anhysteretic susceptibility (χ_y) has several advantages. First, it renders the model immediately applicable to high level recording by use of the whole of the longitudinal anhysteretic curve (Fig. 2a) rather than just the low level linear region. Thus, distortion and saturation effects can be readily examined theoretically. Secondly, the model may be used to study short wavelength bias recording at any signal level. Instead of utilizing the anhysteretic characteristic, one may use the Preisach formalism. This approach has been discussed in relation to a solely longitudinal recording model [7]. However, if one may legitimately neglect the effect of vertical magnetization components even at short wavelengths it may be adapted immediately to include the total vector bias field. The Preisach approach allows the effect of a spread in particle switching fields to be included in a description of the anhysteretic process. Thus, it can provide a usable, complete description of recording at all wavelengths and signal levels.

The neglect of vertical magnetization components may have more fundamental validity than just as a reasonable approximation. The anisotropy of the squareness [8] and anhysteretic susceptibility (unpublished) has been measured on well-oriented tapes. Neither of these quantities may be described by a simple tensor relation: fields applied in the plane of the tape must be at an angle of about 75° to the longitudinal direction before there is appreciable deviation of the remanent magnetization from the alignment direction.

Demagnetization effects due to the tape and head imaging have been neglected since the total field model does such an exceptional job of absolute prediction of long wavelength sensitivity. However, it does seem that strong demagnetization effects should occur. Although the total field model utilizing a finite gap record head explains the average discrepancy (7-8.5 dB) between a longitudinal model and experiment, the deviations are not random. Daniel and Levine's [2] argument for a demagnetization explanation to the discrepancy appears valid, but becomes a second order effect with the good correlation of the total field model. At short wavelength and high signal levels, demagnetizing fields are certainly important. Iwasaki [9] has shown how demagnetizing fields increase the range of switching fields by broadening the recording zone. However, this is only a second order effect in low level, long wavelength recording especially since demagnetization should not alter appreciably the position of the coercivity contour.

Other refinements of the model are possible. For example, the anisotropy of the coercivity could be determined in the recording plane and utilized to find the coercivity contour of any bias setting. Further, a more exact form of the head field function could be incorporated [10]. This would probably improve correlation of the output versus bias curve shape for extremely small coating thickness to gap length ratios.

CONCLUSION

The incorporation of the total vector recording field into a model for low level long wavelength ac bias recording has shown striking improvement in quantitative experimental correlation over a purely longitudinal field model. The present calculation yields an effective anhysteretic susceptibility which is about half of the measured longitudinal susceptibility, thereby removing the major discrepancy between previous theory and experiment. Further, the theory predicts remarkably well the shape of the output vs. bias curve.

It has been argued here that the essential feature of a more accurate modeling of bias recording is the utilization of bias field recording contours which are not necessarily coincident

with those of the predominant signal field. Thus, even though modifications and extensions of the model have been proposed, in particular the inclusion of demagnetizing fields, it appears that the simple model presented here incorporates one of the primary aspects of ac bias recording.

ACKNOWLEDGMENT

The author would like to thank D. Lindholm, J. Mallinson, and J. McKnight for helpful discussions and criticism of the manuscript.

REFERENCES

[1] C. D. Mee, "Physics of Magnetic Recording", North-Holland Publishing Company, 1964.
[2] E. D. Daniel and I. Levine, *J. Acoust. Soc.*, 32, 258-267, 1960; I. Levine and E. D. Daniel, *J. Audio Eng. Soc.*, 7, 181-188, 1959.
[3] See, for example, W. K. Westmijze, *Phillips Res. Rpt.* 8, 245-269, 1953.
[4] H. N. Bertram, *Jour. de Physique Supp.* 32, 684-5, 1970.
[5] O. Karlqvist, *K. Tekn. Hog. Handl.* 86, 1, 1954.
[6] D. L. A. Tjaden and J. Leyten, *Philips Tech. Rev.* 25, 319, 1963.
[7] G. Schwantke, *J. Audio Eng.*, 9, 37, 1961.
[8] H. N. Bertram, *Proc. of AIP, MMM Conf.*, Boston, 1973.
[9] S. Iwasaki, *Ann. of N.Y. Academy of Science*, 189, 3-20, 1972.
[10] See, for example, G. Fan, *IBM Journal*, 321-325, October 1961.

Reprinted by permission from IEEE TRANSACTIONS ON MAGNETICS
Vol. MAG-10, No. 4, December 1974, pp. 1039-1048